Physical Characteristics of Fluidized Beds via Pressure Fluctuation Analysis

Miloslav Hartman and Otakar Trnka
Institute of Chemical Process Fundamentals, Academy of Sciences of the Czech Republic, 165 02 Prague 6-Suchdol, Czech Republic

DOI 10.1002/aic.11518
Published online May 15, 2008 in Wiley InterScience (www.interscience.wiley.com).

During various applications of gas fluidized units, the state/quality of the fluidized bed of solids can change due to changes in operation conditions or variations in the gas or solid feed. An analysis method is developed and applied which employs spectra of the fast Fourier transform of measured pressure fluctuations within the fluidized bed. The procedure is based upon the spectral analysis of successive time series of pressure fluctuations reflecting the actual hydrodynamic state (regime) of the bed. Practical application of the method is illustrated for fluidization at ambient temperature and pressure of spherical particles (glass beads) as well as irregularly shaped particles (limestone, sulfated limestone, and dried sewage sludge), in an 8-cm-ID fluidized bed. Using air, experiments were conducted with different fractions of the materials spanning a very wide range of 0.28–4.5 mm. The evolution was explored of bed behavior from the onset of fluidization to the pneumatic transport (elutriation) of solids from the bed. The method recognizes alterations of the hydrodynamic state of the bed caused by minor changes in the bed mass and/or in the granularity of the bed material. © 2008 American Institute of Chemical Engineers *AIChE J,* 54: 1761–1769, 2008
Keywords: gas–solid fluidization, pressure fluctuations, fluctuation characteristics, behavior of the bed

Introduction

A fluidized bed is one of the types of reactors employed in industry for carrying out gas–solid reactions and physical operations such as drying and granulation.[1,2] Its most important advantages include intensive mixing of the solid particles, the very high bed-to-surface heat transfer, and the fluid-like properties of the gas–solid mixture. Of course, there are also some disadvantages of fluidized beds such as the erosion of bed internals and the loss of very fine particles. Another problem is that because of our limited understanding of the complex hydrodynamics of gas–solid fluidization, reliable control and scale-up of the fluidized bed contact units is still difficult to accomplish.

The hydrodynamic behavior of a fluidized bed varies widely, depending on the particle size distribution, particle density and particle geometry, gas density and gas viscosity, gas flow rate, and column geometry.[3–5] The flow regime or contacting mode changes with increasing gas velocity from incipient fluidization,[6] through bubbling and slugging (small columns only) fluidization, turbulent, and fast fluidization to pneumatic transport.[7,8] General experience indicates that transitions between the different fluidization modes are not usually sharp. A slightly more detailed classification of the fluidization regimes is presented in recent works of ours.[4,9,10] As can be expected, the fluidizing velocity at which major modifications in bed hydrodynamics occur are also affected by pressure and temperature.[11–14]

An intricate, heterogeneous two-phase structure with complicated dynamic changes is the basic characteristic of gas–solid fluidization. Most phenomena occurring in the gas–solid beds can be attributed to the nonlinear interaction between the particles and the gas, which are two very different media with their own individual movement tendencies.[15–17] It is difficult to describe the entangled paths of the two phases. An understanding of the interaction and coupling among random

Correspondence concerning this article should be addressed to M. Hartman at hartman@icpf.cas.cz.

bubble and solid cluster motion, bed oscillations and propagating pressure waves in the fluidized bed may lead to a plausible explanation of complex flow pattern. It is generally accepted that all these phenomena are possible sources of the pressure fluctuations in fluidized gas–solid suspensions.[18]

Pressure fluctuations can also be employed to characterize the quality of fluidization or the performance of a fluidized bed.[19–23] For example, low amplitudes and higher frequencies of the pressure fluctuations tend to manifest the occurrence of small gas pockets (bubbles) or small particle clusters that can lead to intensive heat and mass transfer in the bed.

In this study, the pressure fluctuations were measured under ambient conditions within powder systems comprising diverse particulate materials such as spherical glass beads (ballotini), irregularly shaped limestone and sulfated limestone (calcium sulfate), and fibrous dried sewage sludge. Spectral analysis was employed for the evaluation of the time series of the measured pressure and for monitoring different states of the system, varying from incipient fluidization to considerable entrainment and elutriation. The primary aim of this work was to show that it is also feasible to observe small changes in the size and mass of particles present in the system by means of pressure fluctuations.

Fluctuation Model of a Fluidized Bed

The original model developed in a work of ours[4] has been further extended and modified. It is based upon processing successive time series of the fluctuating pressure signal by means of the fast (discrete) Fourier transform (FFT).

In a period of time of 64 s, a series of pressure data points (P_i) is measured within the bed with a frequency of 512 Hz. Along the measured sequence of P-values as long as 64 s, a time, 4-s long, window is gradually moved with a one-second step. In this way, the original 2048 samples belonging to the time interval 4 s is reduced by successive averaging to 512 samples. The FFT algorithm is applied to the data series of each window. We get 256 values c_i (complex numbers), representing values of the spectral lines from the region of frequencies $f_i \in [f_{\min}, f_{\max}]$, where $f_{\min} = 0.25$ Hz and $f_{\max} = 64$ Hz. The complex spectrum is converted to the amplitude spectrum ($a_i = |c_i|$). Then the lines in the amplitude spectrum are assorted in the degressive order for frequencies between $f_{\min} = 0.25$ Hz and $f_{\max} = 64$ Hz. In addition to the gas superficial velocity, U, two quantities (denoted as M and E) deduced from the assorted amplitude spectrum, were chosen to describe the actual state of the fluidized bed:

(1) The divide ratio of the amplitude spectrum, M, defined as

$$M = 1 - \frac{f_{\mathrm{M}}}{f_{\max}} \tag{1}$$

where the median of the assorted spectrum, f_{M}, is given by

$$f_{\mathrm{M}} = f_{i\mathrm{M}} \tag{2}$$

in which iM complies with

$$\sum_{i=1}^{i\mathrm{M}} a_i = \sum_{i=i\mathrm{M}+1}^{256} a_i \tag{3}$$

Our systematic visual observations and digital camera studies indicate that the fluctuation quantity M is capable of reliable identification of different regimes of the bubbling fluidized beds. The values of M increase from 0.66 to 0.71 for static (fixed) beds with sporadic, small bubbles to 0.96 to 0.99 for large exploding bubbles and/or slugging.

(2) The quantity E is introduced as the square root of the spectral power of the pressure fluctuations in the chosen frequency band, or

$$E = W^{1/2} \tag{4}$$

where

$$W = \frac{4}{256} \cdot \sum_{i=1}^{256} a_i^2 \tag{5}$$

The quantity E can be seen as a measure of the energy dissipated in the bed.

The quantity M, occurring in the interval $M \in < 0.66, 1 >$, can be viewed as a degree of the dominancy of the spectrum.[4] If a measured signal represents a random fluctuating signal, then $M \cong 0.66$. For signals with a single dominant frequency, it holds that $M \to 1$. The values of $M(U)$ and $E(U)$ corresponding to a given superficial gas velocity, U, are computed by averaging the values of M and E of for each 4-s window of the 64-s sequence of data.

The employed model assumes that the actual state of the pressure fluctuations within the fluidized bed can be described by means of three quantities (attractors) $M(U)$, $E(U)$, and the superficial gas velocity, U. This triad defines the position of a "fluctuation" or an "operation" point $\boldsymbol{p} = [M(U), E(U), U]$ in the tridimensional space $\boldsymbol{F} = M \times E \times U$ corresponding to the actual hydrodynamic state of the bed at a given gas velocity, U. When U is systematically varied ($U \in [0, U_{\max}]$), the operation (fluctuation) point moves in space $\boldsymbol{F}$ along curve $\boldsymbol{p} = \mathrm{p}(U)$ called the fluctuation (operation) characteristics of an explored fluidized bed. Projecting this curve to planes $E \times M$ and $E \times U$, we get graphs of the fluctuation characteristics comprising measured data points $\boldsymbol{p}(U_i)$ for $i = 1,2,...n_{\mathrm{exp}}$. The course of the fluctuation characteristics is invariant in time provided that the amount and the quality of the fluidized material remain the same.

Our experience indicates that significant changes in the particulate bed material manifest themselves in relevant changes of the course of the fluidization characteristics. In other words, measured changes in the course of the fluctuation characteristics can warn us about desired or unwanted changes of the bed behavior.

There is ample experimental evidence that the fluidization characteristics (curves) for respective different g-s systems are similar in their mathematical sense. Two characteristics can be transformed, one curve into the other by various transformations of the coordinates U, E, and M. The simplest transformation is the linear one. Our work shows that the linear transformation is capable of describing a number of important and frequent changes of the fluidized beds.

Two different fluctuation characteristics can be compared by a simple linear transformation of one curve into the other.

This can be accomplished by transforming coordinates U, E, and M in the sense of a least-square fit:

$$\overline{U} = \beta \cdot (U - \Delta) \tag{6}$$

$$\overline{E} = E_0 + \alpha \cdot (E - E_0), \tag{7}$$

and

$$\overline{M} = M \tag{8}$$

where E_0 corresponds to the random fluctuating signal of the background, α and β are dilatations of the coordinates of axes E and U, respectively, and Δ is a shift of the origin of axes of the characteristic curve in the direction of axis U.

Experimental

Apparatus

The experiments were performed in a cylindrical glass column of 8 cm ID (d) and a length of 500 cm. The column was equipped with an interchangeable, perforated plate distributor of a free area of 2–12% and orifice diameter of 0.8 mm. All care was taken to ensure uniform gas (air) distribution. The air passed through an oil filter, dryer, and orifice meter or rotameter before it entered the bottom of the column (plenum). The entrained particles were separated in a low-pressure-drop cyclone and, if desired, returned to the column through a fluidized-bed siphon. The superficial velocity of air, U, could be increased up to 4 m s^{-1}. The measurements were carried out at a temperature of 20°C ± 0.5°C and ambient pressure. The height of the fixed (poured) bed varied from 11 to 18 cm.

The pressure within the bed was sampled by a four-mm-ID stainless-steel probe[24–26] located in the bed center at 5 cm above the gas distributor. The outside opening of the probe was connected to a piezoelectric pressure transducer that produced an output voltage proportional to the pressure signal. The output signal, measured relative to the average pressure, was amplified, converted to digital form, and further processed on-line by a personal computer.

Further details on the apparatus, experimental procedure, and fluctuating pressure signal processing by means of fast (discrete) Fourier transform[27] can be found elsewhere.[4,9,10]

Materials used

The present work was conducted with different solids such as ballotini (glass beads), limestone, sulfated limestone (calcium sulfate), and dried sewage sludge. The particulate materials employed belong to Groups B and D powders of the Geldart classification.[3,28] The basic physical properties of the materials used are presented in Tables 1 and 2. It may be of interest to note that the glass beads were near-perfect spheres, the particles of limestone were sharp-edged and of an irregular shape, and the particles of dried sewage sludge were of an irregular shape and fibrous nature. For an overview and characteristics of different operation regimes of fluidized beds such as incipient fluidization, bubbling fluidization, turbulent fluidization and entrainment (fast) fluidization, the reader is referred, for example, to works of ours.[4,9]

Table 1. Tested Solids

Material	Particle Size* d_p (mm)	Mean Particle Size $\bar{d}_p$ (mm)
Ballotini	0.25–0.315	0.28
Ballotini	0.50–0.65	0.57
Ballotini	0.65–0.90	0.77
Ballotini	0.80–1.00	0.90
Ballotini	1.20–1.40	1.30
Dried sewage sludge	0.50–0.80	0.65
Dried sewage sludge	1.0–1.6	1.30
Dried sewage sludge	2.0–2.8	2.40
Dried sewage sludge	4.0–5.0	4.50
Limestone	0.50–0.65	0.57
Sulfated limestone (calcium sulfate)	0.10–0.65	0.37
Sulfated limestone (calcium sulfate)	0.50–0.65	0.57

*Determined by sieving.

Results and Discussion

Influence of the amount of material in the bed

Changes in the amount of material contained in the fluidized bed frequently occur in practice. Such amounts can be expressed as the volume of a fixed (poured, loosely packed) bed or its mass.

Using a very narrow fraction of irregularly shaped limestone particles (0.50–0.65 mm), the fluctuation characteristics were determined for three different masses of the bed: 725, 978, and 1,237 g. Other parameters of the explored beds of these limestone solids are presented in Table 3. As mentioned there, the height of the fixed bed (h) varied from 11 to about 18 cm and the aspect ratio, h/d, increased accordingly from 1.35 to 2.31.

The determined fluctuation characteristics are represented by curves 1–3, shown in Figure 1. As can be seen, the function $E(U)$ is particularly sensitive to changes in the mass of the bed. Since the same size fraction of limestone particles was used in each run, all the curves start in the same point at $U = U_{mf}$. Maxima on the curves $E = E(U)$ indicate the occurrence of turbulent fluidization and considerable expansion (thinning) of the bed. When U attains the value of $U = U_{me}$, a small but significant amount of solids tends to be elutriated from the fluidization column.

In our effort to develop an empirical relationship which would make it possible to transform/converse one curve, $E(U)$, into the other, for a different amount of the identical particles, m, we tested a number of various formulae. On the basis of the experiments with different materials (limestone, glass beads, and dried sewage sludge) we attained the final form of Eq. 9:

$$\frac{E_1(U) - E_0}{E_2(U) - E_0} = \left(\frac{m_1}{m_2}\right)^2 \tag{9}$$

for $U \in [U_{mf}, U_{me}]$.

To obtain the knowledge how good the transformation relationship (9) is, a set of three curves 4 (the thin ones) and 4a (the solid one) are also presented in Figure 1. The thin curves 4 represent the respective conversions (transformations) of experimental curves 1–3 for the chosen mass

Table 2. Physical Properties of Particles

Material	Particle Density, ρ_p (kg m^{-3})	Bulk Density of Loosely Packed Bed (kg m^{-3})	Minimum Fluidization Velocity*, U_{mf} (m s^{-1})
Ballotini	2,510	1,580	0.10–0.84
Dried sewage sludge	990	520	0.32–1.39
Limestone	2,660	1,330	0.25
Sulfated limestone (calcium sulfate)	2,350	1,398	0.11–0.27

*Measured with air under ambient conditions: 21°C, 0.1 MPa.

$m = 1395$ g by means of Eq. 9. As documented by experiment in Figure 1, Eq. 9 is capable of converting the experimental curve $E_i(U)$ measured with m_i into the curve $E_j(U)$ for m_j with good accuracy provided that no particles are elutriated from the vessel, i.e., for $U < U_{me}$. Analogous comparisons made with the other materials (glass beads and dried sewage sludge) provided very similar results.

The exponent on (m_1/m_2) in Eq. 9 was evaluated on the basis of 50 experiments for different materials. The sample variance (the "sample estimate of the population variance"), s^2, indicates that the 95 per cent confidence limits on the exponent on (m_1/m_2) in Eq. 9, based upon the Student/Gosselt/Fisher distribution, are ± 0.0147 or $1.985 \leq$ exponent on $(m_1/m_2) \leq 2.015$. The variance, s^2, amounts to 0.002804 and the absolute systematic error is -0.0032. Thus it can be stated that Eq. 9 enables to estimate quite reliably, for example, the mass of solids that was introduced into or withdrawn or entrained from the bed in the course of operation.

As can be seen in the upper part of Figure 1, the curves $M = M(E)$ exhibit flat maxima, M_{max}, in the range between 0.94 and 0.96. These values slightly increase linearly with the increasing aspect ratio/height of the bed. It should be noted that the quantity M is a measure of dominancy of the amplitude spectrum.[4] Its value suggests whether there are pronounced dominant lines in the spectrum or not. For fluctuations with a single dominant frequency (e.g., slugging), it holds that $M \to 1$. Greater values of M found with higher beds correspond well with general experience. Practice indicates that beds of higher aspect ratios, h/d, have a more pronounced tendency to slugging.

Changes in the bed mass of the same particles are common cases for the linear transformation of the characteristic fluidization curves. Parameters α, β, and Δ occurring in the transformation formulae (6) and (7) can simply be expressed as follows

$$\alpha = \left(\frac{m_1}{m_2}\right)^2, \quad \beta = 1, \quad \text{and} \quad \Delta = 0. \tag{10}$$

Table 3. Different Amounts of Limestone Particles Explored in the Experimental Bed

Run	1	2	3
Mass of particles (g)	725	978	1237
Volume of fixed bed (cm^3)	545	735	930
Height of fixed bed (cm)	10.8	14.6	18.5
Aspect ratio, h/d	1.35	1.82	2.31

Influence of the particle size

The size of the particles contained in the fluidized bed is one of the important quantities that determine the bed behavior (e.g., the points of incipient fluidization and elutriation and the onset of defluidization.)[28] Our practical experience indicates that the fluctuation characteristics change dramatically when the agglomeration of wet/sticky particles occurs in the bed.

Two widely different materials (glass beads/ballotini and dried sewage sludge) were employed to explore the effect of particle size on the fluctuation characteristics. While the first solids are quite heavy and near perfect spheres, the latter of the materials is light and porous with isometric particles of irregular shapes.[29] Narrow fractions of the particles spanning a wide range of 0.28–4.50 mm were used in experiments. The height of the fixed (static) bed of the solids was kept constant at a value of 10 cm in all the experimental runs.

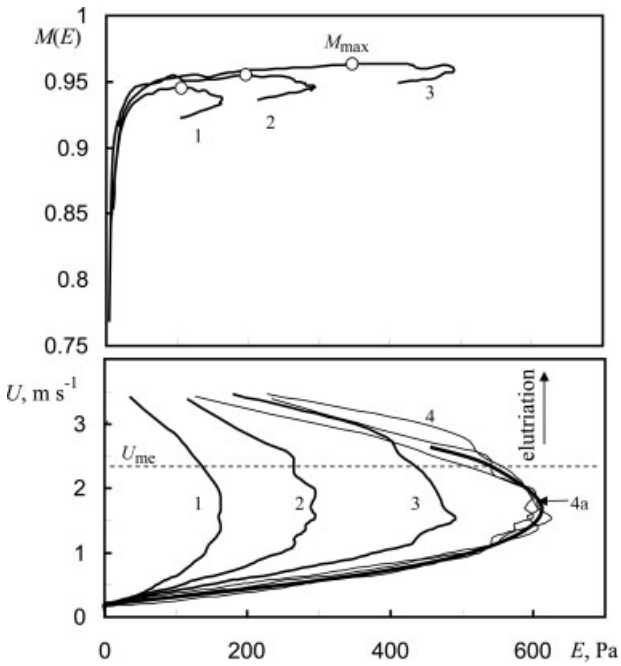

Figure 1. Effect of the mass of the bed, *m*, on its fluctuation characteristics.

Material, limestone; mean particle size, 0.57 mm. Curve 1, $m = 725$ g; curve 2, $m = 978$ g; curve 3, $m = 1237$ g. The points, O, mark maxima, M_{max}, of the function $M(E)$. The set of three thin curves 4 depict the respective conversions (transformations) of experimental curves 1–3 for the chosen mass $m = 1395$ g by means of Eq. 9. The solid line 4a represents the average values of three predictions.

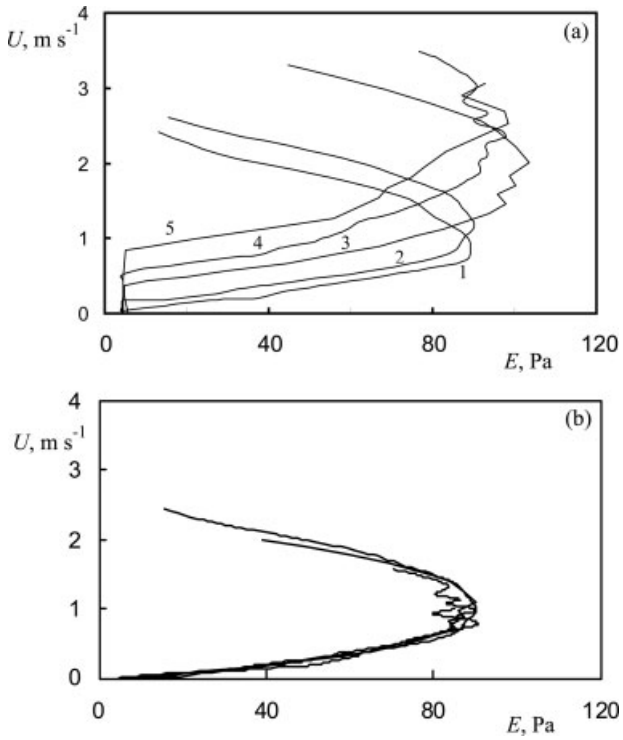

Figure 2. Influence of the mean particle size, $\bar{d}_p$, on the fluctuation characteristics of the bed with glass beads (the height of the fixed [poured] bed: 10 cm).

(a) Curve 1, $\bar{d}_p$ = 0.28 mm; curve 2, $\bar{d}_p$ = 0.57 mm; curve 3, $\bar{d}_p$ = 0.77 mm; curve 4, $\bar{d}_p$ = 0.90 mm; curve 5, $\bar{d}_p$ = 1.30 mm; (b) fluctuation characteristics after the linear transformations; all the curves (1–5) were linearly transformed to curve 2, depicted by a darker line.

As can be seen in Figures 2 and 3 (section [a]), the size of the solids affects markedly the course of the fluctuation characteristics $E(U)$ of both materials. It appears that the influence of $\bar{d}_p$ on $E(U)$ is especially remarkable with the relatively light particles of dried sewage sludge.

The characteristic functions $E(U)$ of the beds with different fractions of the same material can be mutually transformed with the aid of linear relationships (6)–(8) including parameters α, β, and Δ. The results of such transformations are also shown in Figures 2 (ballotini) and 3 (dried sewage sludge) in section (b). As visual observations suggest, the fluctuation characteristics $E(U)$ are well transformable for the different sized fractions of the given solids.

The determined values of parameters α, β, and Δ for the respective fractions of the two materials are presented in Table 4. Parameter Δ is strongly dependent on the mean size of particles in the bed and represents the minimum fluidization velocity of the bed material in question. The point of minimum fluidization, U_{mf}, was also determined by the standard procedure of measuring the dependence of the bed pressure drop on the air flow with the air velocity gradually reduced from a well-fluidized state to a fixed (packed, static) bed.[6] The measured values of U_{mf} were in good agreement with the corresponding values of parameter Δ presented in Table 4.

Parameter β that represents the dilatation of axis U is also significantly dependent upon the particle size. Parameter α, representing the dilatation of axis E does not change much (from 0.95 to 1.14) with $\bar{d}_p$. In other words, it means that the maximum of the function $E(U)$ for a given material is only slightly dependent on the particle size of bed material.

The dependencies of the aforementioned parameters on the particle size for the two explored materials are shown in Figures 4 and 5. To have a full picture, the dependence of the maximum value of the function $M(E)$, M_{max}, on $\bar{d}_p$ is also shown in Figures 4 and 5. As can be seen, this maximum increases slightly with the increasing particle size. In other words, the tendency of the fluidized bed to slug is more pronounced with larger particles. This is in accord with the general experience.

Elutriation from beds and their fluctuation characteristics

On increasing the gas velocity through the column, the flow in the bed shifts from the bubbling regime to the turbulent regime, a further increase in gas flow rate leads to fast fluidization and transport. In practical applications it is

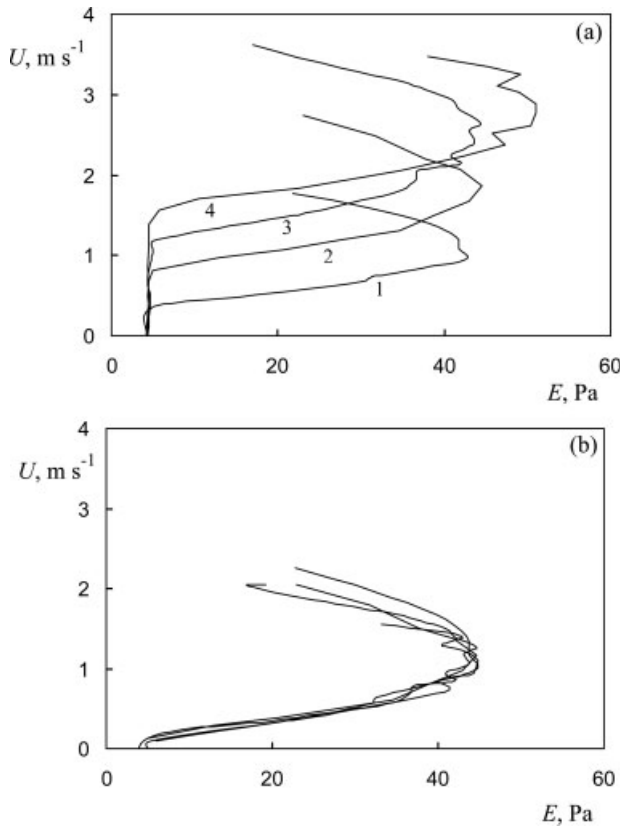

Figure 3. Influence of the mean particle size, $\bar{d}_p$, on the fluctuation characteristics of the bed with particles of dry sewage sludge (the height of the fixed [poured] bed: 10 cm).

(a) Curve 1, $\bar{d}_p$ = 0.65 mm; curve 2, $\bar{d}_p$ = 1.3 mm; curve 3, $\bar{d}_p$ = 2.4 mm; curve 4, $\bar{d}_p$ = 4.5 mm; (b) fluctuation characteristics after the linear transformations: all the curves (1–4) were linearly transformed to curve 2, depicted by a darker line.

Table 4. Parameters of the Linear Transformations of the Fluctuation Characteristics

Mean Particle Size (mm)	Material: Ballotini* $\Delta \cong U_{mf}$ (m s^{-1})	α	β
0.28	0.10	0.99	1.10
0.57	0.18	1.00	1.00
0.77	0.43	1.15	0.70
0.90	0.53	1.09	0.53
1.30	0.84	1.09	0.45
Mean Particle Size (mm)	**Material: Dried sewage sludge† $\Delta \cong U_{mf}$ (m s^{-1})**	**α**	**β**
0.65	0.32	0.956	1.55
1.30	0.69	1.000	1.00
2.40	1.07	0.997	0.80
4.50	1.39	1.145	0.75

*Near spherical, nonporous particles.
†Irregularly shaped, porous, fibrous particles.[29]

commonplace for solids to be blown from a fluidized bed into the freeboard space above it. This phenomenon is known as entrainment[1] and it becomes more severe as the superficial gas velocity, U, increases. The solids thrown up into the freeboard space contain the whole spectrum of particle sizes present in the bed. If "U" equals the terminal (free fall) velocity[7,8] of the smaller particles, these solids will be elutriated,[1] i.e., carried out of the fluidization column (system) completely, whereas the larger particles fall back to the bed surface. In other words, the particles elutriated from the system are only those of which the terminal (free fall) velocity, U_t, is less than the superficial gas velocity, U, in the vessel. In essence, the phenomenon of elutriation affects the bed in two different ways: It reduces the mass of the bed and simultaneously shifts the size distribution of the bed material towards coarser particles.

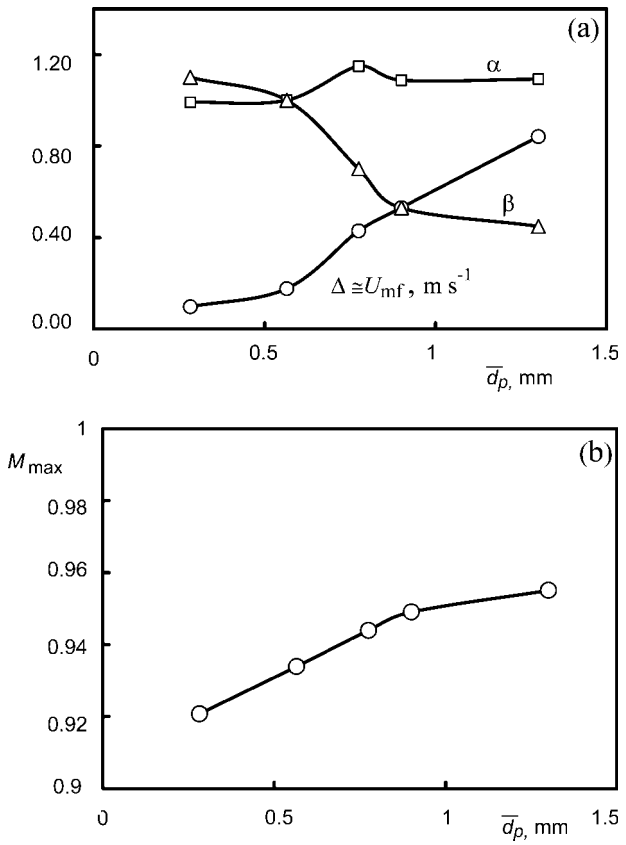

Figure 4. Dependencies of parameters α, β, and Δ of the linear transformations of the fluctuation characteristics on the mean particle size of the bed material (glass beads/ballotini).

(a) Parameters α, β, and Δ; (b) dependency of the maximum of the quantity $M(U)$.

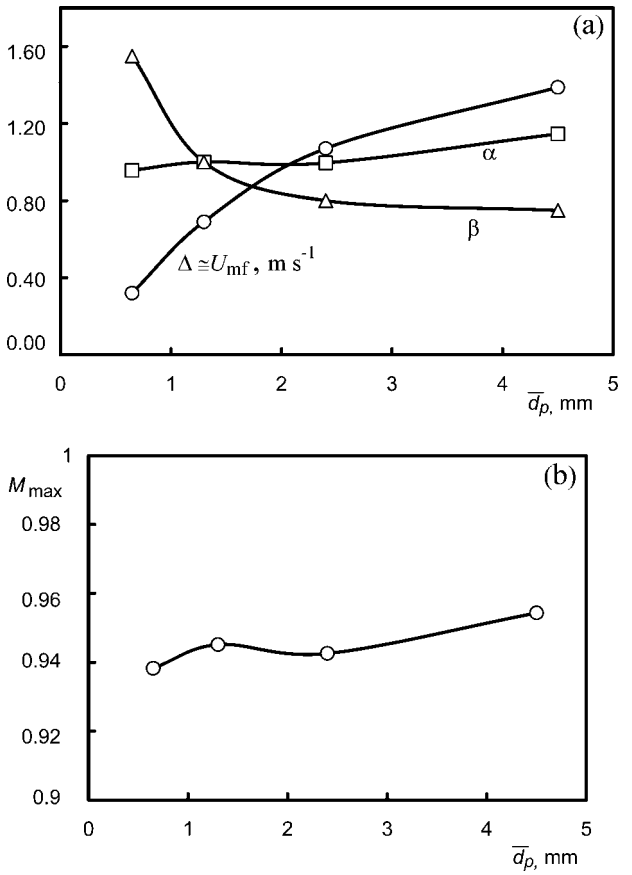

Figure 5. Dependencies of parameters α, β, and Δ of the linear transformations of the fluctuation characteristics on the mean particle size of the bed material (dried sewage sludge).

(a) Parameters α, β, and Δ; (b) dependency of the maximum of the quantity $M(U)$.

The elutriation experiments, whose results are presented in Figure 6, were performed as follows. A mass (760 g) of particles of calcium sulfate spanning a wider size range of 0.10–0.65 mm was introduced into the column. The superficial velocity of air was gradually increased from zero through the onset of fluidization, $U_{mf} = 0.11$ m s^{-1}, to the onset of elutriation, $U_{me} = 1.25$ m s^{-1}, where dilute transport flow (DTF) commenced/occurred. This procedure is represented by curve 1 in Figure 6. Consequently, the mass of the bed was reduced due to the elutriation of finer particles and the quantity $E(U)$ decreased, although U was kept constant. This

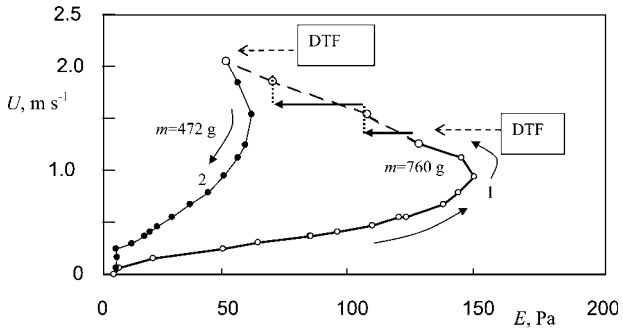

Figure 6. Impact of particle elutriation from the fluidized bed on its fluctuation characteristics.

Bed material, calcium sulfate; ○, characteristic curve 1 for the bed of initial mass of 760 g with 0.1–0.65 mm particles; the onset of fluidization, $U_{mf} = 0.11$ m s^{-1}; the onset of elutriation, $U_{me} = 1.25$ m s^{-1}; ●, characteristic curve 2 for the bed reduced by the elutriation of smaller particles; bed mass, 472 g; particle size, 0.50–0.65 mm; the onset of fluidization, $U_{mf} = 0.27$ m s^{-1}; the onset of elutriation, $U_{me} = 2.06$ m s^{-1}; DTF (dilute transport flow).

is shown by an arrow in Figure 6. In general, the elutriation practically ceased after 8–10 min of fluidizing under given conditions (U = const.). When the elutriation was completed, the air flow rate was increased by a suitable increment and the procedure was repeated. In dilute transport flow, the characteristic curve $E(U)$ has a stepwise character that depends on the time schedule of incremental changes of the air flow rate, U. When the value of $U = 2.06$ m s^{-1} was attained, the air velocity was not increased further. The mass of the final (remaining) bed amounted to 472 g and contained a narrow fraction of larger particles (0.50–0.65 mm) whose U_{mf} was as large as 0.27 m s^{-1}.

The fluctuation characteristics of the aforementioned, new bed ($m = 472$ g, $\bar{d}_p = 0.50$–0.65 mm) was also determined for $U \in (U_{mf} = 0.27$ m s^{-1}, $U_{me} = 2.06$ m s$^{-1})$. It is represented by curve 2, also shown in Figure 6. As can be seen, curve 1 and curve 2 share one common point at $U = 2.06$ m s^{-1} but their courses are markedly different. While curve 2 is not affected by elutriation, curve 1 includes the influence of elutriation for $U \in (1.25, 2.06$ m s$^{-1})$.

Utilizing differences in the courses of the two fluctuation curves in Figure 6, we can determine the amount of the bed material (smaller particles) that left the fluidization column. Furthermore, we are also able to estimate quite reliably the onset of fluidization of the new (remaining) bed and the mean particle size of the material in this bed. Each of the two curves can be transformed linearly into the other curve. The procedure of transformation is visualized in Figure 7 and consists of the following steps:

Step 1: A shift of curve 2 along coordinate U to reach a coincidence of the outsets of fluidization of the two characteristics. The length of this shift is given as

$$\Delta = U_{mf}^{\text{curve 2}} - U_{mf}^{\text{curve 1}} \tag{11}$$

Step 2: A linear dilatation of curve 2 in the direction of axis U. The coefficient of dilatation β is determined so that the two curves could attain the maximum $E(U)$ at approximately the same value of U. An overall transformation of coordinate U, composed of the two partial ones, can be written in the form

$$\overline{U} = \Delta + \beta \cdot (U - \Delta) \tag{12}$$

Step 3: A linear dilatation of the coordinate is given as

$$\overline{E} = E_0 + \alpha \cdot (E - E_0) \tag{13}$$

where α is found so that maxima of the functions $E^{\text{curve 1}}(U)$ and $E^{\text{curve 2}}(U)$ are as close as possible. E_0 represents a position of the ever-present background of quantity E.

We are aiming at a linear transformation of the coordinates so that the resulting function $E(U)$ can approximate as closely as possible (in the sense of a minimum sum of the squares of the deviations) a corresponding section of the original curve $E(U)$. In this way, an optimization process is defined for fitting the three parameters, α, β, and Δ to the measured data. For the aforementioned characteristics, optimized values of the respective parameters were found as large as $\alpha = 2.49$, $\beta = 0.67$, and $\Delta = 0.16$ m s^{-1}.

Via physical interpretation of these parameters, we get the properties of the new (remaining) bed after elutriation as follows:

(1) On inserting $\alpha = 2.49$ into Eq. 10, we can estimate the mass of the bed remaining in the vessel after elutriation:

$$m^{\text{curve 2}} = m^{\text{curve 1}} \cdot \frac{1}{\alpha^{0.5}} = \frac{810.8}{2.49^{0.5}} = 513.8 \text{ g} \tag{14}$$

This predicted value compares quite well with the mass of the new bed determined by weighing (503.3 g).

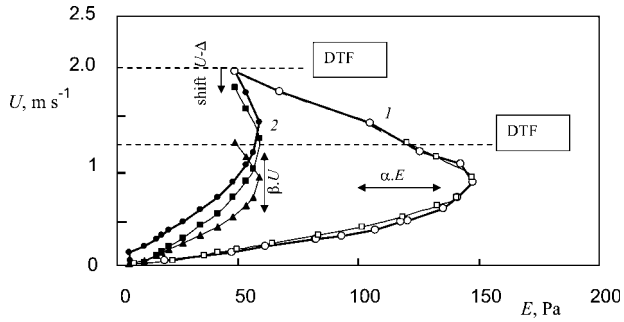

Figure 7. Procedure for transforming characteristic curve 2 (the bed reduced by elutriation, m = 472 g) to a curve comparable with original curve 1 (the initial bed, m = 760 g).

Bed material, calcium sulfate; ○, curve 1, characteristic curve for the original (initial) bed ($m = 760$ g, $\bar{d}_p = 0.1$–0.65 mm) after a shift along the U-axis by $\Delta U = -0.11$ m s^{-1}; then the onset of fluidization is zero in this drawing; ●; curve 2, the characteristic curve of the bed reduced by elutriation ($m = 472$ g) $\bar{d}_p = 0.5$–0.65 mm; the curve is shifted along the U-axis by $\Delta U = -0.11$ m s^{-1}; then the onset of fluidization is 0.16 m s^{-1} in this drawing. Procedure for linear transformation: ■, curve 2 shifted along the U-axis by its onset of fluidization, $\Delta = 0.16$ m s^{-1}; ▲, dilatation of coordinate U by parameter $\beta = 0.67$; □, dilatation of coordinate E by multiplying $\alpha = 2.49$.

(2) Parameter Δ makes it possible to determine the onset of fluidization of the new bed after elutriation

$$\overline{U}_{\mathrm{mf}} = U_{\mathrm{mf}} + \Delta = 0.11 + 0.16 = 0.27 \text{ m s}^{-1} \qquad (15)$$

This point of minimum fluidization is in very good agreement with that determined by independent experiment.

(3) From the fact that the transformed curve $\overline{E}(U)$ approximates the original characteristic curve 1 in Figure 7 very well, it can be stated that all the onsets of operation regimes and subregimes[4] of fluidized beds have these functions identically. On combining Eqs. 11 and 12 we can develop Eq. 16 to approximately predict the aforementioned onsets of different regimes and subregimes (e.g., onsets of turbulence and elutriation) of a resulting bed from the values of these onsets determined for the original (initial) bed:

$$U_{\mathrm{onset}}^{\mathrm{curve\ 2}} = \frac{U_{\mathrm{onset}}^{\mathrm{curve\ 1}} - U_{\mathrm{mf}}^{\mathrm{curve\ 1}}}{\beta} + U_{\mathrm{mf}}^{\mathrm{curve\ 1}} \qquad (16)$$

Having inserted the values $U_{\mathrm{mf}}^{\mathrm{curve\ 1}} = 0.11$ m s^{-1}, $U_{\mathrm{me}}^{\mathrm{curve\ 1}} = 1.25$ m s^{-1}, and $\beta = 0.67$ into Eq. 16, we get $U_{\mathrm{me}}^{\mathrm{curve\ 2}} = 1.81$ m s^{-1} for the onset of elutriation of the new bed. This prediction is in fair agreement with the experiment (2.06 m s^{-1}).

Postlude

We wish to emphasize that the proposed method is based on a large volume of carefully performed experimental work with a bench-scale fluidization column and with various particulate materials. Of course the transformation parameters, presented here for Group B and D particles of the Geldart classification, have the usual limitations. They should be applied with caution outside the experimental conditions from which they were educed. The method is being employed with success to determine and monitor the state of a high-temperature bed in our 0.3 m $\times$ 0.3 m $\times$ 4.5 m fluidized combustor.

Conclusions

It has been demonstrated that the fluctuation characteristics of different fluidized beds $E(U)$ deduced from experimental measurements can be linearly transformed into each other with the aid of three parameters (α, β, and Δ). Having had these parameters, we can quite easily and reliably predict, for example, the differences in the mass, the onset of fluidization, and the onset of elutriation of particles from the bed. These findings serve as a physically solid basis for the instrumental identification and control of the state of a fluidized bed. With respect to its technical simplicity, this technique is particularly promising for high-temperature fluidized bed processes.

Acknowledgments

The authors gratefully acknowledge the financial support provided for this work by GA AS ČR (Grant IAA 400720701).

Notation

a_i = amplitude pertaining to i-line of spectrum
c_i = complex value pertaining to i-line of spectrum
d = diameter of bed (cm)
d_{p} = particle size (determined by sieving) (mm, m)
$\bar{d}_{\mathrm{p}}$ = mean particle size (mm, m)
DTF = dilute transport flow
$E(U)$ = characteristic quantity of pressure fluctuations defined by Eq. 4 (Pa)
$\overline{E}$ = transformed quantity E defined by Eq. 7
E_0 = quantity E corresponding to the random fluctuating signal of the background (Pa)
f_i = frequency pertaining to i-line of amplitude spectrum (Hz)
f_{M} = median of assorted spectrum (Hz)
$f_{\max}$ = maximum frequence of discrete Fourier spectrum (Hz)
$f_{\min}$ = minimum frequency of discrete Fourier spectrum (Hz)
$\boldsymbol{F}$ = tridimensional space $E \times M \times U$
FFT = fast (discrete) Fourier transform
h = height of static bed (cm)
i = index of line in amplitude spectrum
m = mass of bed (g, kg)
$M(U)$ = characteristic quantity of pressure fluctuations defined by Eq. 1
$\boldsymbol{p}$ = fluctuation state vector [$E(U)$, $M(U)$, U]
P = pressure (Pa)
U = superficial gas velocity (m s^{-1})
$\bar{U}$ = transformed superficial gas velocity defined by Eq. 6
$U_{\max}$ = maximum superficial gas velocity (m s^{-1})
U_{me} = onset of elutriation (determined by visual observations) (m s^{-1})
U_{mf} = onset of fluidization (m s^{-1})
U_{t} = terminal (free fall) velocity (m s^{-1})
W = spectral power of fluctuations (Pa^2)

Greek letters

α = dilatation of coordinates of the axis U
β = dilatation of coordinates of the axis E
Δ = shift of the origin of axes of the characteristic curve in the direction of axis U
ρ = bulk density of loosely packed (poured) bed of particles (kg m^{-3})
ρ_{p} = particle (apparent, mercury) density (kg m^{-3})

Literature Cited

1. Yates JG. *Fundamentals of Fluidized-Bed Chemical Procsses*. London: Butterworths, 1983.
2. Chaplin G, Pugsley T, Winters C. Application of chaos analysis to pressure fluctuation data from a fluidized bed dryer containing pharmaceutical granule. *Powder Technol*. 2004;142:110–120.
3. Hartman M, Beran Z, Svoboda K, Veselý V. Operation regimes of fluidized beds. *Collect Czech Chem Commun*. 1995;60:1–33.
4. Trnka O, Veselý V, Hartman M, Beran Z. Identification of the state of a fluidized bed by pressure fluctuations. *AIChE J*. 2000;46:509–514.
5. Andreux R, Gauthier T, Chaouki J, Simonin O. New description of fluidization regimes. *AIChE J*. 2005;51:1125–1130.
6. Hartman M, Coughlin RW. On the incipient fluidized state of solid particles. *Collect Czech Chem Commun*. 1993;58:1213–1241.
7. Hartman M, Yates JG. Free-fall of solid particles through fluids. *Collect Czech Chem Commun*. 1993;58:961–982.
8. Hartman M, Trnka O, Svoboda K. Free-settling of nonspherical particles. *Ind Eng Chem Res*. 1994;33:1979–1983.
9. Trnka O, Hartman M, Veselý V. Characteristics of pressure fluctuations in different operation regimes of gas-solid suspensions. *Chem Listy*. 2005;99:330–338.
10. Trnka O, Hartman M. Influence of changes in physical parameters of fluidized beds on its characteristics of pressure fluctuations. *Chem Listy*. 2007;101:515–523.
11. Chen A, Bi HT. Pressure fluctuations and transition from bubbling to turbulent fluidization. *Powder Technol*. 2003;133:237–246.
12. Svoboda K, Čermák J, Hartman M, Drahoš J, Selucký K. Pressure fluctuations in gas-fluidized beds at elevated temperatures. *Ind Eng Chem Process Dev*. 1983;22:514–520.

13. Guo Q, Yue G, Werther J. Dynamics of pressure fluctuation in a bubbling fluidized bed at high temperature. *Ing Eng Chem Res*. 2002;41:3482–3488.
14. Guo Q, Yue G, Suda T, Sato J. Flow characteristics in a bubbling fluidized bed at elevated temperature. *Chem Eng Proces*. 2003;42: 439–447.
15. Zhao G-B, Yang Y-R. Multiscale resolution of fluidized-bed pressure fluctuations. *AIChE J*. 2003;49:869–882.
16. Hao B, Bi HT. Forced bed mass oscillations in gas-solid fluidized beds. *Powder Technol*. 2005;149:51–60.
17. Wu B, Kantzas A, Bellehumeur CT, He Z, Kryuchkov S. Multiresolution analysis of pressure fluctuations in a gas-solids fluidized bed: application to glass beads and polyethylene powder systems. *Chem Eng J*. 2007;131:23–33.
18. Bi HT. A critical review of the complex pressure fluctuation phenomenon in gas-solids fluidized beds. *Chem Eng Sci*. 2007;62:3473–3493.
19. Svoboda K, Čermák J, Hartman M, Drahoš J, Selucký K. Influence of particle size on the pressure fluctuations and slugging in a fluidized bed. *AIChE J*. 1984;30:513–517.
20. Schouten JC, van den Bleek CM. Monitoring the quality of fluidization using the short-term predictability of pressure fluctuations. *AIChE J*. 1998;44:48–60.
21. Van Ommen JR, Coppens M-O, van den Bleek CM, Schouten JC. Early warning of agglomeration in fluidized beds by attractor comparison. *AIChE J*. 2000;46:2183–2197.
22. Van der Schaaf J, van Ommen JR, Takens F, Schouten JC, van den Bleek CM. Similarity between chaos analysis and frequency analysis of pressure fluctuations in fluidized beds. *Chem Eng Sci*. 2004;59: 1829–1840.
23. Croxford AJ, Gilbertson MA. Control of the state of a bubbling fluidized bed. *Chem Eng Sci*. 2006;61:6302–6315.
24. Yates JG, Simons SJR. Experimental methods in fluidization research. *Int J Multiphase Flow*. 1994;20:297–330.
25. Xie H-Y, Geldart D. The response time of pressure probes. *Powder Technol*. 1998;95:185–204.
26. Werther J. Measurement techniques in fluidized bed. *Powder Technol*. 1999;102:15–36.
27. Press WH, Flannery BP, Teukolsky SA, Vetterling WT. *Numerical Recipes in Pascal*. Cambridge: Cambridge University Press, 1992.
28. Geldart D. Types of fluidization. *Powder Technol*. 1973;7:285–292.
29. Hartman M, Pohořelý M, Trnka O. Fluidization of dried wastewater sludge. *Powder Technol*. 2007;178:166–172.

Manuscript received Nov. 14, 2007, and revision received Apr. 7, 2008.